HHS Public Access

Author manuscript

Science. Author manuscript; available in PMC 2017 July 26.

Published in final edited form as:

Science. 2016 March 18; 351(6279): 1329–1333. doi:10.1126/science.aaf1648.

Tuft cells, taste-chemosensory cells, orchestrate parasite type 2 immunity in the gut

Michael R. Howitt[1], **Sydney Lavoie**[1], **Monia Michaud**[1], **Arthur M. Blum**[2], **Sara V. Tran**[3], **Joel V. Weinstock**[2], **Carey Ann Gallini**[1], **Kevin Redding**[3], **Robert F. Margolskee**[3], **Lisa C. Osborne**[4,*], **David Artis**[4], and **Wendy S. Garrett**[1,5,6,†]

[1]Departments of Immunology and Infectious Diseases and Genetics and Complex Diseases, Harvard T. H. Chan School of Public Health, Boston, MA 02115, USA

[2]Division of Gastroenterology, Tufts Medical Center, Boston, MA 02111, USA

[3]Monell Chemical Senses Center, Philadelphia, PA 19104, USA

[4]Jill Roberts Institute for Research in Inflammatory Bowel Disease, Weill Cornell Medical College, Cornell University, New York, NY 10021, USA

[5]Broad Institute of Harvard and Massachusetts Institute of Technology, Cambridge, MA 02142, USA

[6]Department of Medical Oncology, Dana-Farber Cancer Institute, Boston, MA 02215, USA

Abstract

The intestinal epithelium forms an essential barrier between a host and its microbiota. Protozoa and helminths are members of the gut microbiota of mammals, including humans, yet the many ways that gut epithelial cells orchestrate responses to these eukaryotes remain unclear. Here we show that tuft cells, which are taste-chemosensory epithelial cells, accumulate during parasite colonization and infection. Disruption of chemosensory signaling through the loss of TRMP5 abrogates the expansion of tuft cells, goblet cells, eosinophils, and type 2 innate lymphoid cells during parasite colonization. Tuft cells are the primary source of the parasite-induced cytokine interleukin-25, which indirectly induces tuft cell expansion by promoting interleukin-13 production by innate lymphoid cells. Our results identify intestinal tuft cells as critical sentinels in the gut epithelium that promote type 2 immunity in response to intestinal parasites.

The mammalian gut microbiota is a collective of bacteria, archaea, viruses, fungi, and parasites that reside in the lumen and mucosal surface of the intestine. These microbes are

†Corresponding author. wgarrett@hsph.harvard.edu.

*Present address: Department of Microbiology and Immunology, University of British Columbia, Vancouver, British Columbia V6T 1Z3, Canada.

The authors declare no competing financial interests.

SUPPLEMENTARY MATERIALS

www.sciencemag.org/content/351/6279/1329/suppl/DC1

Materials and Methods

Figs. S1 to S13

References (*49–53*)

sequestered from interior tissues by a single layer of epithelial cells lining the gut that acts as a barrier and sensor. Intestinal epithelial cells (IECs) express pattern recognition receptors that detect microbial components and thus are critical sensors for and orchestrators of mucosal immunity (1–4).

Beyond pattern recognition receptors, hosts monitor and respond to the microbiota via heterotrimeric guanine nucleotide–binding protein (G protein)–coupled receptors (GPCRs). For example, microbially produced short-chain fatty acids are sensed via GPR41 and GPR43 (5,6), and sinonasal epithelial cells can detect the pathogen *Pseudomonas aeruginosa* via a taste-chemosensory GPCR (7–12). Many taste-chemosensory GPCRs require the taste-specific G protein subunit gustducin and the cation channel TRPM5 to transduce their signals (7,9). The disruption of either gustducin or TRPM5 can perturb physiological responses to *P. aeruginosa* (13–15). In the gut, TRPM5 and other canonical taste-chemosensory components are predominantly expressed by an intestinal epithelial subset called tuft cells (16). Tuft cells, which are identified by the expression of doublecortin-like kinase 1 (DCLK1), comprise a minor fraction of small intestinal epithelial cells (17–19) and are putative quiescent stem cells (20). Although tuft cells express taste-chemosensory machinery, it is unknown whether tuft cells sense the gut microbiota by means of taste chemosensation or transduce signals to the mucosal immune system (21).

We began by evaluating the frequency of $DCLK1^+$ tuft cells in the distal small intestine of wild-type (WT) specific-pathogen-free mice that were bred in-house (BIH). We found markedly more intestinal $DCLK1^+$ tuft cells (7.2%) (Fig. 1A) than previous reports (0.4%) (19,22) and confirmed this discrepancy with an alternative tuft cell marker, GFI1B (fig. S1) (23). As interinstitutional differences in microbiota can contribute to substantial variation among mucosal immune cell populations (24), we compared tuft cell abundance in mice obtained from The Jackson Laboratory (JAX) with BIH mice. Similar to previous reports (19,25), tuft cells constituted 1.0% of the total IEC population of JAX mice (Fig. 1A). Feeding the cecal contents from BIH mice to JAX mice was sufficient to increase tuft cell populations to BIH levels (fig. S2), suggesting that transmissible components of the BIH microbiota may drive tuft cell expansion when introduced to JAX mice. In support of this idea, intestinal histology revealed numerous single-celled protozoa in BIH but not in JAX mice (Fig. 1B). To identify these protozoa, we purified and imaged them by means of scanning electron microscopy (SEM); we identified them as tritrichomonads (Fig. 1C) (26–28). Quantitative polymerase chain reaction (qPCR) confirmed that they were *Tritrichomonas muris* (Tm), a common but understudied member of the rodent microbiota (Fig. 1D).

To eradicate Tm from BIH mice, we added metronidazole (2.5 g/liter) to their drinking water for 1 week. This eliminated Tm and concomitantly reduced tuft cell abundance (fig. S3). Because this treatment does not exclude the possibility that other metronidazole-sensitive organisms may contribute to tuft cell expansion, we cultured Tm (28,29) and colonized unexposed mice. Tm colonization significantly elevated tuft cell numbers in conventional (Fig. 1, E and F) and germ-free mice (fig. S4), suggesting that this symbiotic protozoa is sufficient to increase tuft cell frequency.

Helminths are common eukaryotic inhabitants of the mammalian intestine, but they are evolutionarily distinct from protozoa. These parasites inflict a substantial global health burden, yet worms may also provide therapeutic benefits (8). To investigate the effect of helminth infection on tuft cell abundance, we infected mice with a diverse set of parasitic worms including *Heligmosomoides polygyrus* (Hp), *Trichinella spiralis* (Ts), and *Nippostrongylus brasiliensis* (Nb). Similar to our results with Tm, infections with all three helminths increased tuft cell abundance, indicating that expansion of tuft cells is a broadly conserved feature of parasite colonization (Fig. 1, G and H).

Because tuft cells are postulated to be chemosensory cells (30), we considered whether perturbations to tuft chemosensory pathways may affect their expansion in response to parasites and/or to the type 2 immune response typically initiated by parasites. Multiple taste-chemosensory GPCRs sense sweet, bitter, and umami compounds; engagement of these different receptors activates a common signal transduction pathway involving gustducin, PLCβ2, and TRPM5 (Fig. S5) (7, 9). We confirmed that GFI1B^{+} tuft cells are the primary IEC subset expressing the canonical taste-associated components gustducin, PLCβ2, and TRPM5 (Fig. 2A) (16, 23, 31).

We compared tuft cell abundance in WT and gustducin-deficient (*gustducin*$^{-/-}$) mice colonized with Tm and found significantly fewer tuft cells in *gustducin*$^{-/-}$ animals (Fig. 2B). Using *Trpm5*^{eGFP} (eGFP, enhanced green fluorescent protein) reporter mice, we validated that TRPM5 is restricted to the epithelium and expressed by DCLK1^{+} tuft cells in the distal small intestine (Fig. 2C and fig. S6). Given the multiplicity of taste-chemosensory GPCRs, the established role of TRPM5 in taste chemosensation (7,32), and the predominant intestinal TRPM5 expression by tuft cells, we used TRPM5-deficient mice to evaluate whether these pathways affect tuft cell parasite responses. Similar to *gustducin*$^{-/-}$ mice, tuft cells failed to expand in *Trpm5*$^{-/-}$ mice during Tm colonization (Fig. 2, D to F). To determine whether the blunted response was due to reduced parasite colonization, we measured Tm in the distal small intestine (fig. S7A). We found slightly more parasites in both *gustducin*$^{-/-}$ and *Trpm5T*$^{-/-}$ mice than in WT mice (fig. S7B), indicating that the lack of tuft cell response was not due to decreased Tm colonization. Because Tm is a stable component of the microbiota, we tested how the loss of TRPM5 would affect clearance of a pathogenic helminth such as Hp. Thirty-six days after infection, we determined that *Trpm5*$^{-/-}$ mice had a significantly higher worm burden than WT mice (fig. S7C). Collectively, these data suggest that pathways initiated upstream of TRPM5 may mediate tuft cell responses to intestinal parasites.

If tuft cell responses represent an early step in parasite recognition, we hypothesized that other antiparasitic responses may be altered in parasite-burdened *Trpm5*$^{-/-}$ mice. Consistent with helminth infections (33), Tm colonization also induced goblet cell hyperplasia in WT ($P < 0.0001$) but not in *Trpm5*$^{-/-}$ mice (Fig. 2, G and H). Similarly, we observed eosinophilia in WT but not in *Trpm5*$^{-/-}$ mice colonized with Tm (Fig. 2I).

Because epithelial cells are a key source of the parasite-induced cytokines thymic stromal lymphopoietin (TSLP) and interleukin-33 (IL-33) and -25 (17), we isolated tuft cells and the remaining epithelial fraction to determine TSLP, IL-33, and IL-25 expression patterns.

Consistent with recent reports, we found that tuft cells expressed less TSLP and IL-33 than other epithelial cells and are the main source of epithelial IL-25 (Fig. 3A and fig. S8A) (34,35). To determine whether TRPM5 affects parasite-induced IL-25 expression, we infected WT and *Trpm5*$^{-/-}$ mice with Tm and measured both parasite colonization and the corresponding epithelial IL-25 expression over time. Tm rapidly colonized both WT and *Trpm5*$^{-/-}$ mice, but *Trpm5*$^{-/-}$ mice had significantly reduced IL-25 expression 12 days after infection ($P = 0.0006$) (Fig. 3B).

IL-25 promotes proliferation and activation of type 2 innate lymphoid cells (ILC2s) via the receptor subunit IL17RB (11, 36,37). Accordingly, the frequency of intestinal lamina propria IL17RB^{+} ILC2s significantly increased in WT but not *Trpm5*$^{-/-}$ mice after 12 days of Tm infection (Fig. 3C). To determine whether the parasite response in *Trpm5*$^{-/-}$ mice could be complemented by exogenous IL-25, we injected IL-25 intraperitoneally into *Trpm5*$^{-/-}$ mice; we observed restoration of distal small intestinal eosinophilia and tuft cell abundance (Fig. 3, D to F), suggesting that tuft cells may influence their own abundance.

Epithelial cells are not only a crucial source of IL-25 but also signal in an autocrine manner via IL17RB (22). Therefore, we examined tuft cell IL17RB expression and found that it was significantly higher ($P = 0.0043$) than for other epithelial cells (fig. S8B). This raised the question of whether IL-25 induces tuft cell expansion via autocrine signaling or indirectly through recruitment of ILC2s. To evaluate factors that affect tuft cell abundance independently of the microbiota or immune system, we used an in vitro primary intestinal organoid system (38,39). Small intestinal organoids reconstitute all the epithelial subsets from IEC stem cells. By generating organoids from *Gfi1b*$^{eGFP/+}$ mice, we detected GFP^{+} tuft cells (Fig. 4A and fig. S9A). Both WT and *Trpm5*$^{-/-}$ organoids contained ~0.3% tuft cells, but IL-25 did not increase tuft cell numbers (Fig. 4B and fig. S9A), suggesting that IL-25 does not act in an autocrine manner to expand tuft cell abundance. Because IL-25 promotes expansion of ILC2s, which are critical sources of IL-13 (11,36,40), a cytokine previously shown to increase goblet cell numbers (25), we considered that IL-13 may also increase tuft cell abundance. IL-13 significantly expanded tuft cells from 0.3% of total organoid cells to 11.9% and 10.9% (WT and *Trpm5*$^{-/-}$, respectively) (Fig. 4B and fig. S9A). In agreement with these results, expression of DCLK1 and TRPM5 also increased in IL-13-treated organoids (fig. S9, B and C).

To determine whether type 2 cytokine production by ILC2s may contribute to tuft cell expansion in vivo, we colonized WT, *Stat6*$^{-/-}$, *Rag2*$^{-/-}$, and *Rag2*$^{-/-}$*Il2rγ*$^{-/-}$ mice with Tm (fig. S10). STAT6 is activated by the type 2 cytokines IL-4 and IL-13 and is required for intestinal helminth expulsion (26). Consistent with our organoid data demonstrating that IL-13 potently induces tuft cell expansion, tuft cells did not expand when Tm colonized *Stat6*$^{-/-}$ mice (Fig. 4, C and D). Although both T helper 2 (T_H2) and ILC2 cells can produce IL-13 in mucosal tissue (41), parasite-induced IL-25 potently activates IL-13 expression in ILCs (11,36,42). We compared tuft cell abundance in *Rag2*$^{-/-}$ mice that lack T_H2 cells but contain ILC2s versus *Rag2*$^{-/-}$*Il2rγ*$^{-/-}$ mice that lack both T_H2 and ILC2s cells (8,11,12). Infected *Rag2*$^{-/-}$ mice had elevated tuft cell abundance compared with uninfected WT mice; however, similar to both *Trpm5*$^{-/-}$ and *Stat6*$^{-/-}$ mice, *Rag2*$^{-/-}$*Il2rγ*$^{-/-}$ mice showed no tuft cell increase during Tm infection (Fig. 4, C and D). Collectively, these data suggest that tuft

cells may detect Tm through TRPM5 taste chemosensation to elicit ILCs, which in turn produce IL-13 to expand tuft cell abundance (fig. S11).

IECs are positioned for direct contact with lumenal microbes and microbial products, and they function as sensory nodes to promote homeostasis with symbiotic microbes and initiate immunity against pathogens. Eukaryota, including helminths and protozoa, are common members of the gut microbiota (43, 44) that profoundly modulate the host immune system (45,46). Many of the pattern recognition receptor systems that recognize bacterial members of the microbiota do not contribute to recognition of parasites (47,48). Here we show that tuft cells orchestrate type 2 immunity, in agreement with two recent studies (34,35). Taste receptors respond to a panoply of ingested agonists (18), and we speculate that tuft cells and taste chemosensation within the gut provide similarly broad recognition of parasitic signals.

Supplementary Material

Refer to Web version on PubMed Central for supplementary material.

Acknowledgments

We thank members of the Garrett Lab for helpful discussion, T. Stappenbeck for supplying L-WRN cells, R. Montgomery for help with organoid imaging, and W. Fowle for help with SEM. The data from this study are tabulated in the main paper and in the supplementary materials. *Trpm5*^{eGFP}, *Trpm5*$^{-/-}$, and *gustducin*$^{-/-}$ mice are available from Monell Chemical Senses Center under a material transfer agreement. This work was supported by NIH National Research Service Award (NRSA) F32DK098826 to M.R.H.; NIH NRSA F31DK105653 to S.L.; and NIH grants R01 CA154426 and R01 GM099531, a Burroughs Wellcome Career in Medical Sciences Award, and a Searle Scholars Award to W.S.G.

REFERENCES AND NOTES

1. Kobayashi KS, et al. Science. 2005; 307:731–734. [PubMed: 15692051]
2. Rakoff-Nahoum S, Paglino J, Eslami-Varzaneh F, Edberg S, Medzhitov R. Cell. 2004; 118:229–241. [PubMed: 15260992]
3. Vaishnava S, Behrendt CL, Ismail AS, Eckmann L, Hooper LV. Proc Natl Acad Sci USA. 2008; 105:20858–20863. [PubMed: 19075245]
4. Vaishnava S, et al. Science. 2011; 334:255–258. [PubMed: 21998396]
5. Smith PM, et al. Science. 2013; 341:569–573. [PubMed: 23828891]
6. Kim MH, Kang SG, Park JH, Yanagisawa M, Kim CH. Gastroenterology. 2013; 145:396–406.e10. [PubMed: 23665276]
7. Zhang Y, et al. Cell. 2003; 112:293–301. [PubMed: 12581520]
8. Mishra PK, Palma M, Bleich D, Loke P, Gause WC. Mucosal Immunol. 2014; 7:753–762. [PubMed: 24736234]
9. Wong GT, Gannon KS, Margolskee RF. Nature. 1996; 381:796–800. [PubMed: 8657284]
10. Lee RJ, et al. J Clin Invest. 2012; 122:4145–4159. [PubMed: 23041624]
11. Huang Y, et al. Nat Immunol. 2015; 16:161–169. [PubMed: 25531830]
12. Hurst SD, et al. J Immunol. 2002; 169:443–453. [PubMed: 12077275]
13. Tizzano M, et al. Proc Natl Acad Sci USA. 2010; 107:3210–3215. [PubMed: 20133764]
14. Lee RJ, et al. J Clin Invest. 2014; 124:1393–1405. [PubMed: 24531552]
15. Saunders CJ, Christensen M, Finger TE, Tizzano M. Proc Natl Acad Sci USA. 2014; 111:6075–6080. [PubMed: 24711432]
16. Bezenpon C, et al. J Comp Neurol. 2008; 509:514–525. [PubMed: 18537122]
17. Peterson LW, Artis D. Nat Rev Immunol. 2014; 14:141–153. [PubMed: 24566914]

18. Meyerhof W, et al. Chem Senses. 2010; 35:157–170. [PubMed: 20022913]
19. Gerbe F, et al. J Cell Biol. 2011; 192:767–780. [PubMed: 21383077]
20. Westphalen CB, et al. J Clin Invest. 2014; 124:1283–1295. [PubMed: 24487592]
21. Gerbe F, Legraverend C, Jay P. Cell Mol Life Sci. 2012; 69:2907–2917. [PubMed: 22527717]
22. Kang Z, et al. Immunity. 2012; 36:821–833. [PubMed: 22608496]
23. Bjerknes M, et al. Dev Biol. 2012; 362:194–218. [PubMed: 22185794]
24. Ivanov II, et al. Cell. 2009; 139:485–498. [PubMed: 19836068]
25. McKenzie GJ, Bancroft A, Grencis RK, McKenzie ANJ. Curr Biol. 1998; 8:339–342. [PubMed: 9512421]
26. Urban JF Jr, et al. Immunity. 1998; 8:255–264. [PubMed: 9492006]
27. Baker, DG. Flynn's Parasites of Laboratory Animals. Baker, DG., editor. Blackwell Publishing; 2008. p. 303-397.
28. Materials and methods are available as supplementary materials on *Science* Online
29. Saeki H, Togo M, Imai S, Ishii T. Japan J Vet Sci. 1983; 45:151–156.
30. Schütz B, et al. Front Physiol. 2015; 6:87. [PubMed: 25852573]
31. Kusumakshi S, et al. Chem Senses. 2015; 40:413–425. [PubMed: 25940069]
32. Pérez CA, et al. Nat Neurosci. 2002; 5:1169–1176. [PubMed: 12368808]
33. Khan WI, Blennerhasset P, Ma C, Matthaei KI, Collins SM. Parasite Immunol. 2001; 23:39–42. [PubMed: 11136476]
34. von Moltke J, Ji M, Liang HE, Locksley RM. Nature. 2016; 529:221–225. [PubMed: 26675736]
35. Gerbe F, et al. Nature. 2016; 529:226–230. [PubMed: 26762460]
36. Neill DR, et al. Nature. 2010; 464:1367–1370. [PubMed: 20200518]
37. Saenz SA, et al. Nature. 2010; 464:1362–1366. [PubMed: 20200520]
38. Miyoshi H, Stappenbeck TS. Nat Protoc. 2013; 8:2471–2482. [PubMed: 24232249]
39. Sato T, et al. Nature. 2009; 459:262–265. [PubMed: 19329995]
40. Fallon PG, et al. J Exp Med. 2006; 203:1105–1116. [PubMed: 16606668]
41. Liang HE, et al. Nat Immunol. 2012; 13:58–66.
42. Price AE, et al. Proc Natl Acad Sci USA. 2010; 107:11489–11494. [PubMed: 20534524]
43. Parfrey LW, et al. Front Microbiol. 2014; 5:298. [PubMed: 24995004]
44. Hotez PJ, et al. J Clin Invest. 2008; 118:1311–1321. [PubMed: 18382743]
45. Osborne LC, et al. Science. 2014; 345:578–582. [PubMed: 25082704]
46. Reese TA, et al. Science. 2014; 345:573–577. [PubMed: 24968940]
47. Helmby H, Grencis RK. Eur J Immunol. 2003; 33:2974–2979. [PubMed: 14579265]
48. Reynolds LA, et al. J Immunol. 2014; 193:2984–2993. [PubMed: 25114104]

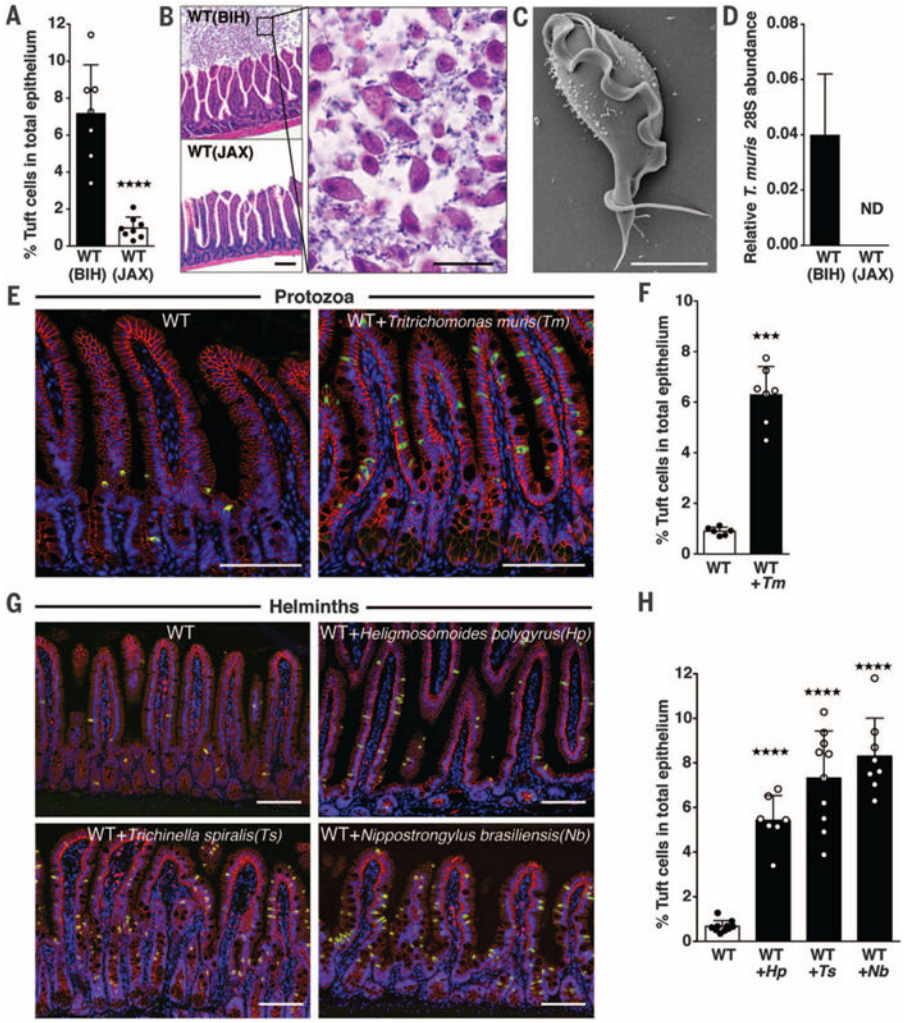

Fig. 1. Symbiotic protozoa or helminths increase intestinal tuft cell abundance

(**A**) DCLK1^{+} tuft cell frequency in the small intestine (SI) of WT BIH and WT JAX mice. (**B**) Hemtoxylin and eosin-stained SI sections from WT BIH and WT JAX mice (scale bar, 50 μm) (left). A higher magnification of the WT BIH section is shown on the right (scale bar, 20 μm). (**C**) SEM micrograph of protozoa isolated from WT BIH mice (scale bar, 4 μm). (**D**) Tm abundance in stool DNA (Tm 28S rRNA relative to Eubacteria 16S rRNA), determined by qPCR (ND, not detectable). (**E**) Representative SI images from uninfected and Tm-colonized mice and (**F**) tuft cell frequency. (**G**) Representative SI images from uninfected and helminth-colonized mice and (**H**) tuft cell frequency. DCLK1 is shown in green, E-cadherin in red, and DAPI (4′,6-diamidino-2-phenylindole) in blue [scale bars in (E) and (G), 100 μm]. Each symbol represents an individual mouse, and all data are representative of two [(D), (F), and (H)] or three (A) independent experiments. Tm infection was 17 days in (E) and (F). In (G) and (H), Hp infection was 21 days, Ts infection was 15 days, and Nb infection was 8 days. Data are plotted as means with SD. Four stars, $P < 0.0001$; three stars, $P = 0.0001$; one-way analysis of variance (ANOVA) or Mann-Whitney test.

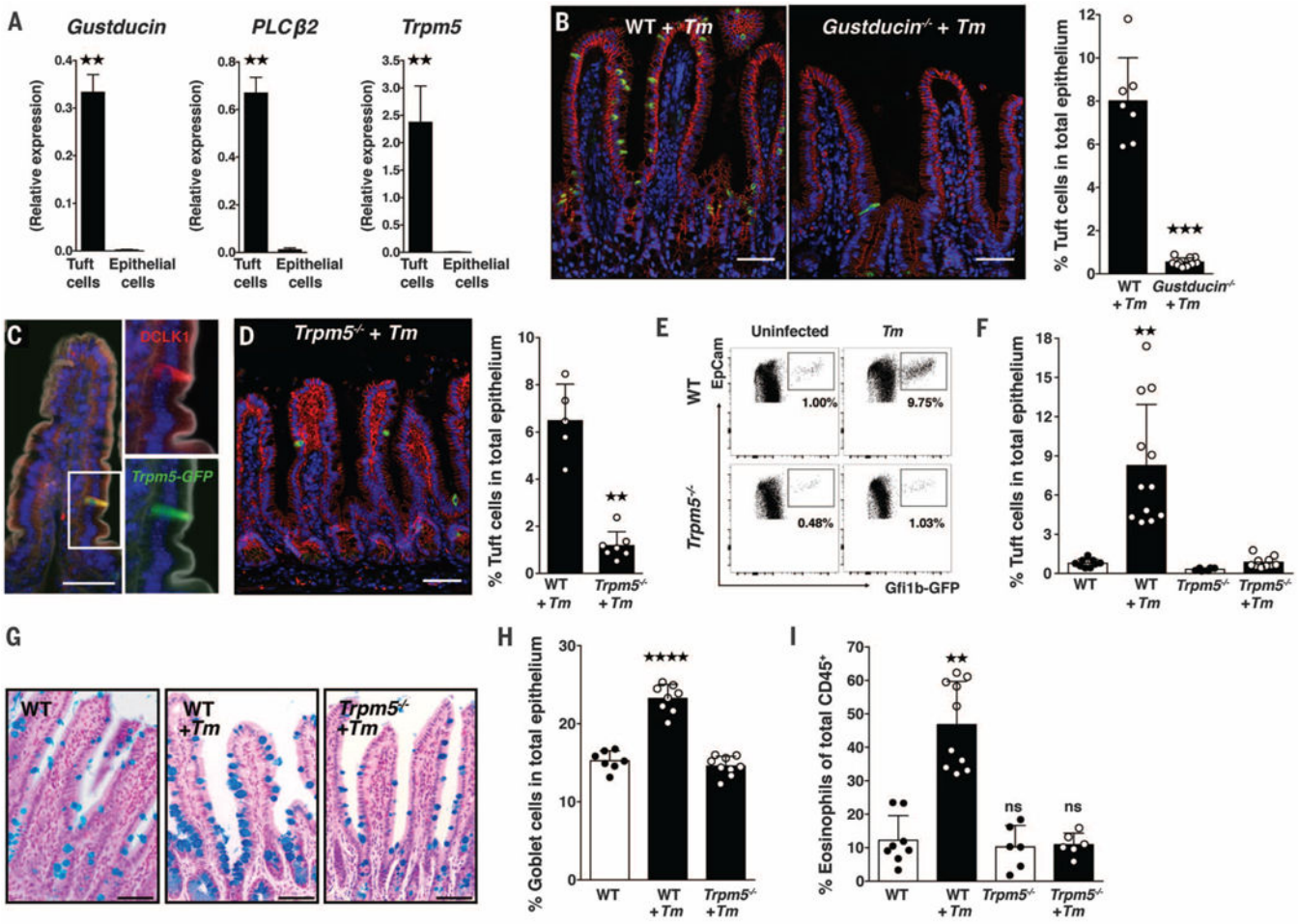

Fig. 2. Tuft cells influence type 2 immunity through TRPM5

(**A**) Gustducin, PLCβ2, and TRPM5 expression in sorted tuft cells, compared with the non-tuft cell epithelium. (**B**) Representative images of Tm-colonized WT and *gustducin*$^{-/-}$ mice and tuft cell frequencies. (**C**) Representative image from *Trpm5*^{eGFP} mice. GFP is shown in green), DCLK1 in red), DAPI in blue, and phalloidin in white. (**D**) Representative image of Tm-colonized *Trpm5*$^{-/-}$ mice and tuft cell frequencies. Scale bars in (B), (C), and (D), 50 μm. (**E**) Representative flow cytometry plots of IECs from uninfected (left) or Tm-colonized (right) WT (*Gfi1b*$^{eGFP/+}$, top) and *Trpm5*$^{-/-}$ (*Gfi1b*$^{eGFP/+}$ *Trpm5*$^{-/-}$, bottom) mice and (**F**) tuft cell frequency. (**G**) Goblet cells in SI sections stained with Alcian blue and nuclear red in uninfected WT and Tm-colonized WT and *Trpm5*$^{-/-}$ mice and (**H**) goblet cell frequency. (**I**) Eosinophil frequency in the distal SI lamina propria (LP) of uninfected and Tm-colonized WT and *Trpm5*$^{-/-}$ mice. Scale bars, 50 μm. Each symbol represents an individual mouse, and all data are representative of at least three independent experiments. Data are plotted as means with SD. Four stars, $P < 0.0001$; three stars, $P = 0.0001$; two stars, $P < 0.01$; ns, not significant; one-way ANOVA, Kruskal-Wallis, or Mann-Whitney tests.

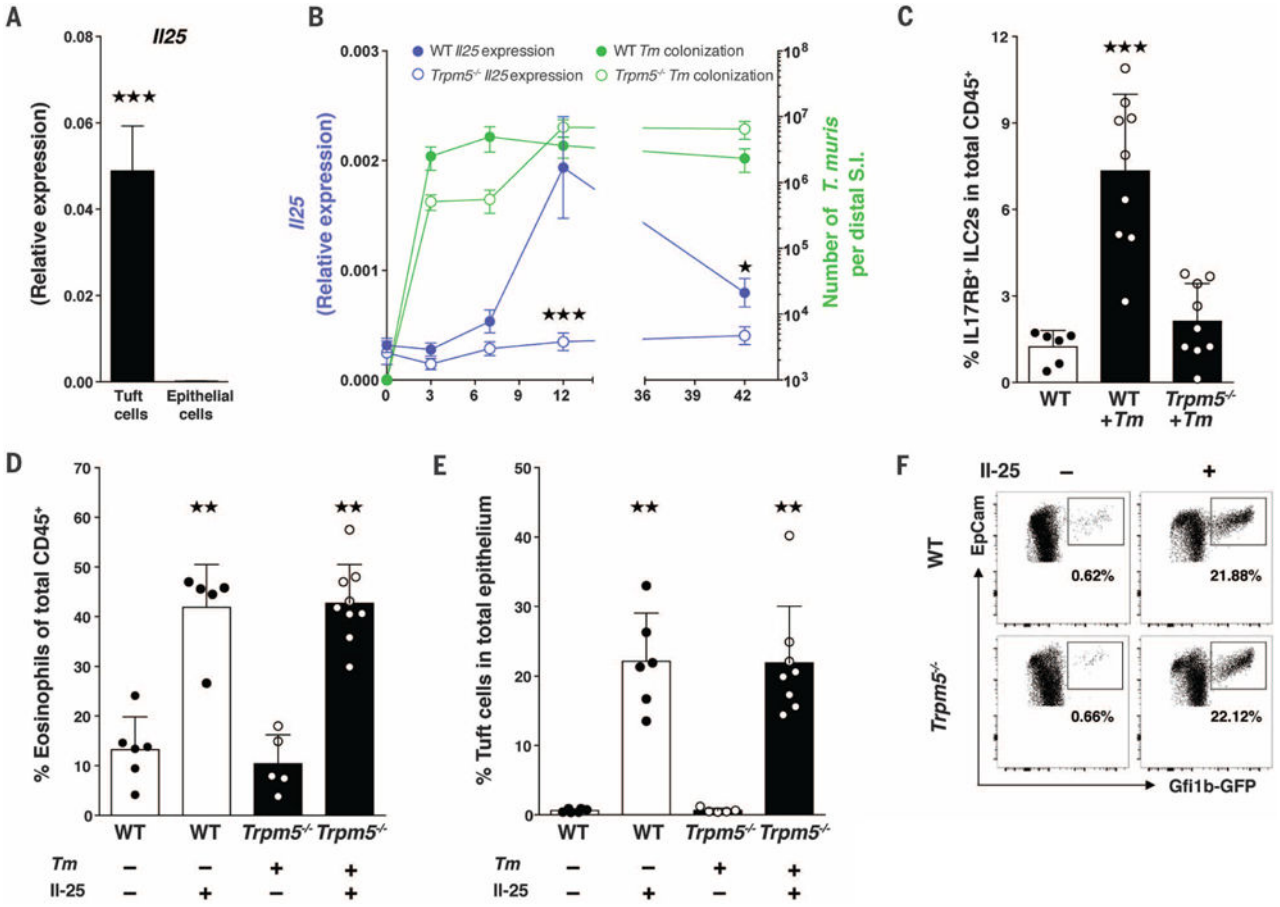

Fig. 3. Tuft cells express IL-25 and elicit ILC2s in a TRPM5-dependent manner in response to symbiotic protozoa

(**A**) IL-25 expression from sorted tuft cells. (**B**) WT (solid circles) and *Trpm5*$^{-/-}$ (open circles) mice were colonized with Tm for 3, 7, 12, and 42 days. At each time point, epithelial cell IL-25 expression was measured (purple line) and Tm colonization was quantified (green line). (**C**) Frequency of IL17RB^{+} (IL-25R) ILC2s in the distal SI LP of uninfected WT mice and WT and *Trpm5*$^{-/-}$ mice colonized with Tm for 12 days. (**D**) Eosinophil frequency in the distal SI LP of uninfected WT or Tm-colonized *Trpm5*$^{-/-}$ mice intraperitoneally injected with IL-25 or phosphate-buffered saline (PBS) control. (**E**) Tuft cell frequencies and (**F**) flow plots of epithelial cells isolated from *Trpm5*$^{-/-}$ mice intraperitoneally injected with IL-25 or PBS. Each symbol in (C), (D), and (E) represents an individual mouse, and all data are representative of three independent experiments. Data are plotted as means with SD.Three stars, $P < 0.001$; two stars, $P < 0.01$; Kruskal-Wallis or Mann-Whitney tests.

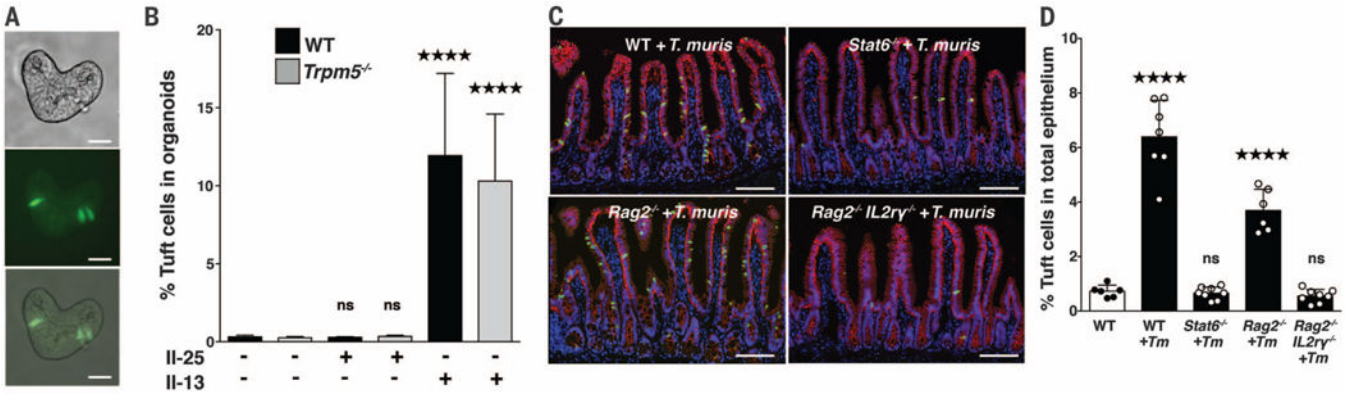

Fig. 4. Innate lymphoid cells and IL-13 increase tuft cells in organoids and the small intestine

(**A**) Differential interference contrast, fluorescent, and merged images of small intestinal organoids generated from *Gfi1b*$^{eGFP/+}$ mice (scale bars, 25 μm). (**B**) GFP^{+} tuft cell abundance by flow cytometry of WT and *Trpm5*$^{-/-}$ organoids treated with recombinant IL-13 or IL-25. (**C**) Representative images of SI from WT, *Stat6*$^{-/-}$, *Rag2*$^{-/-}$, and *Rag2*$^{-/-}$*Il2rγ*$^{-/-}$ mice colonized with Tm and (**D**) tuft cell frequency. DCLK1 is shown in green, E-cadherin in red, and DAPI in blue (scale bars, 100 μm). Each symbol in (D) represents an individual mouse, and all data are representative of (D) two or (B) three independent experiments. Data are plotted as means with SD. Four stars, $P < 0.0001$; one-way ANOVA or Mann-Whitney tests.